

Small molecules enhance autophagy and reduce toxicity in Huntington's disease models

Sovan Sarkar^{1,6}, Ethan O Perlstein^{2,3,6}, Sara Imarisio⁴, Sandra Pineau¹, Axelle Cordenier⁴, Rebecca L Maglathlin³, John A Webster³, Timothy A Lewis³, Cahir J O'Kane⁴, Stuart L Schreiber^{3,5} & David C Rubinsztein¹

The target of rapamycin proteins regulate various cellular processes including autophagy¹, which may play a protective role in certain neurodegenerative and infectious diseases². Here we show that a primary small-molecule screen in yeast yields novel small-molecule modulators of mammalian autophagy. We first identified new small-molecule enhancers (SMER) and inhibitors (SMIR) of the cytostatic effects of rapamycin in *Saccharomyces cerevisiae*. Three SMERs induced autophagy independently of rapamycin in mammalian cells, enhancing the clearance of autophagy substrates such as mutant huntingtin and A53T α -synuclein, which are associated with Huntington's disease and familial Parkinson's disease, respectively^{3–5}. These SMERs, which seem to act either independently or downstream of the target of rapamycin, attenuated mutant huntingtin-fragment toxicity in Huntington's disease cell and *Drosophila melanogaster* models, which suggests therapeutic potential. We also screened structural analogs of these SMERs and identified additional candidate drugs that enhanced autophagy substrate clearance. Thus, we have demonstrated proof of principle for a new approach for discovery of small-molecule modulators of mammalian autophagy.

The autophagy/lysosome and ubiquitin/proteasome pathways are the two main routes for protein clearance in eukaryotic cells. Proteasomes predominantly degrade short-lived nuclear and cytosolic proteins, which need to be unfolded to pass through the narrow pore of the proteasome barrel, thereby precluding clearance of large membrane proteins and protein complexes (including oligomers and aggregates). Mammalian lysosomes, on the other hand, can degrade substrates such as protein complexes and organelles. The bulk degradation of cytoplasmic proteins and organelles is largely mediated by macroautophagy, generally referred to as autophagy¹. It involves the formation of double-membrane structures called autophagosomes or autophagic vacuoles, which fuse with lysosomes to form autolysosomes (also called autophagolysosomes), where their contents are

degraded by acidic lysosomal hydrolases. Autophagosomes are generated by elongation of small membrane structures whose precise origins have yet to be elucidated¹. Autophagy can be induced under physiological stress conditions such as starvation. Several protein kinases regulate autophagy, the best characterized being the mammalian target of rapamycin (mTOR), which negatively regulates the pathway in organisms from yeast to humans¹. However, the targets of mTOR-dependent and mTOR-independent signaling in the autophagy apparatus are not well understood in mammalian systems. Recently, we described an mTOR-independent pathway in which autophagy is induced by agents that lower inositol (1) or inositol-1,4,5-triphosphate (IP₃) (2) concentrations⁶.

Autophagy is an important process in a variety of human diseases caused by toxic, aggregate-prone, intracytosolic proteins, which become inaccessible to the proteasome when they oligomerise^{2–5}. These include Huntington's disease (HD), an autosomal-dominant neurodegenerative disorder caused by a CAG trinucleotide repeat expansion (>35 repeats) that encodes an abnormally long polyglutamine (polyQ) tract in the N terminus of the huntingtin protein⁷. Mutant huntingtin toxicity is thought to be exposed after it is cleaved to form N-terminal fragments comprising the first 100–150 residues with the expanded polyQ tract, which are also the toxic species found in aggregates. Thus, HD pathogenesis is frequently modeled with exon 1 fragments containing expanded polyQ repeats that cause aggregate formation and toxicity in cell models and *in vivo*⁷.

In addition to mutant huntingtin, autophagy also regulates the clearance of other aggregate-prone disease-causing proteins, such as those causing spinocerebellar ataxia type 3, forms of tau (which cause fronto-temporal dementias) and the A53T and A30P α -synuclein mutants (which cause familial Parkinson's disease (PD))^{3–6,8,9}. Autophagy induction reduces mutant huntingtin levels and protects against its toxicity in cell, *D. melanogaster* and mouse models^{3,4}. Similar effects are seen with other polyQ-containing proteins and tau in cells and flies⁹. Certain bacterial and viral infections may also be treatable by autophagy upregulation, because the pathogens can be engulfed by autophagosomes and transferred to lysosomes for degradation. These

¹Department of Medical Genetics, University of Cambridge, Cambridge Institute for Medical Research, Addenbrooke's Hospital, Hills Road, Cambridge CB2 2XY, UK.

²Department of Molecular and Cellular Biology, Harvard University, 7 Divinity Avenue, Cambridge, Massachusetts 02138, USA. ³Howard Hughes Medical Institute, the Broad Institute of Harvard and MIT, 7 Cambridge Center, Cambridge, Massachusetts 02142, USA. ⁴Department of Genetics, University of Cambridge, Cambridge CB2 3EH, UK. ⁵Department of Chemistry and Chemical Biology, Harvard University, 12 Oxford Street, Cambridge, Massachusetts 02138, USA. ⁶These authors contributed equally to this work. Correspondence should be addressed to S.L.S. (stuart_schreiber@harvard.edu) or D.C.R. (dcr1000@cam.ac.uk).

Received 14 February; accepted 16 April; published online 7 May 2007; doi:10.1038/nchembio883

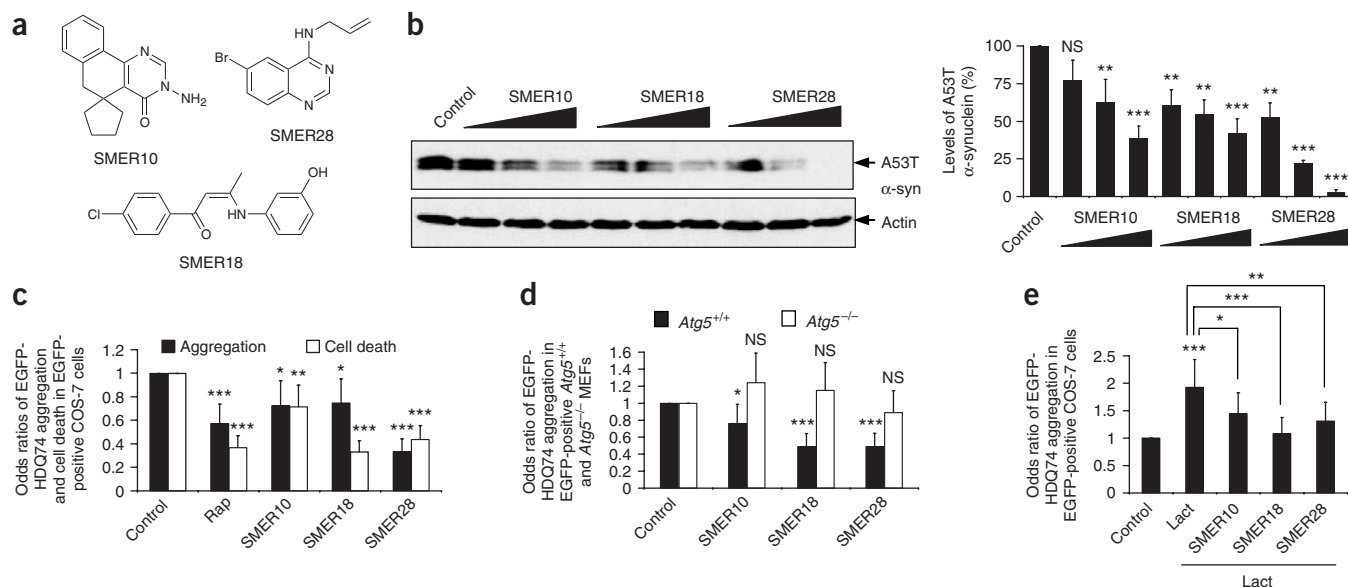


Figure 1 SMERs 10, 18 and 28 enhance the clearance of mutant aggregate-prone proteins by autophagy in mammalian cell models of Huntington's and Parkinson's disease, independent of rapamycin. **(a)** Chemical structures of SMERs 10, 18 and 28. **(b)** A53T α -synuclein (α -syn) expression was induced in stable PC12 cells for 48 h, then switched off for 24 h. Cells were treated with DMSO (control), or with 0.94 μ M, 4.7 μ M or 47 μ M of SMER10; 0.86 μ M, 4.3 μ M or 43 μ M of SMER18; or 0.9 μ M, 4.7 μ M or 47 μ M of SMER28 added in the switch-off period. A53T α -syn levels were analyzed by immunoblotting with antibody against HA (left) and densitometry analysis relative to actin (right). Error bars denote s.e.m. $P = 0.0917$, $P = 0.009$, $P = 0.0001$ (for increasing concentrations of SMER10); $P = 0.0068$, $P = 0.0023$, $P = 0.0002$ (for increasing concentrations of SMER18); $P = 0.0016$, $P < 0.0001$, $P < 0.0001$ (for increasing concentrations of SMER28). **(c)** COS-7 cells transfected with EGFP-HDQ74 construct were treated with DMSO (control), 0.2 μ M rapamycin (Rap), 47 μ M SMER10, 43 μ M SMER18 or 47 μ M SMER28 for 48 h, and we assessed the proportions of apoptotic or aggregate-containing transfected cells. Error bars: 95% confidence interval. $P < 0.0001$ (Rap and SMER28), $P = 0.013$ (SMER10), $P = 0.019$ (SMER18) (aggregation); $P < 0.0001$ (Rap, SMER18 and SMER28), $P = 0.004$ (SMER10) (cell death). **(d)** Wild-type (*Atg5*^{+/+}) and knockout (*Atg5*^{-/-}) *Atg5* MEFs were transfected with EGFP-HDQ74 and treated with DMSO (control), 47 μ M SMER10, 43 μ M SMER18 or 47 μ M SMER28 for 24 h, and we assessed the percentages of aggregate-containing transfected cells. The control (DMSO-treated) values were fixed at 1 for both cell lines. Error bars: 95% confidence interval. $P = 0.039$ (SMER10), $P < 0.0001$ (SMER18 and SMER28) (in *Atg5*^{+/+} cells); $P = 0.092$ (SMER10), $P = 0.271$ (SMER18), $P = 0.358$ (SMER28) (in *Atg5*^{-/-} cells). Note that EGFP-HDQ74 aggregation was higher in *Atg5*^{-/-} than in *Atg5*^{+/+} cells (**Supplementary Fig. 3a**). **(e)** The percentages of EGFP-positive COS-7 cells with EGFP-HDQ74 aggregates as in **c**, treated with DMSO (control), 10 μ M lactacystin (proteasome inhibitor) or both 10 μ M lactacystin along with either 47 μ M SMER10, 43 μ M SMER18 or 47 μ M SMER28 for 48 h, expressed as odds ratios. Error bars: 95% confidence interval. $P < 0.0001$ (control versus Lact), $P = 0.014$ (SMER10 versus Lact), $P < 0.0001$ (SMER18 versus Lact), $P = 0.001$ (SMER28 versus Lact). *** $P < 0.001$; ** $P < 0.01$; * $P < 0.05$; NS, nonsignificant.

include *Mycobacterium tuberculosis* (which causes tuberculosis), group A *Streptococcus* and viruses such as herpes simplex virus type 1 (refs. 2,10–12).

Currently, the only small molecule known to upregulate autophagy in mammalian brains is rapamycin (3), which, when complexed to its intracellular binding protein FKBP12, is a specific TOR inhibitor^{2,4}. However, TOR proteins control several cellular processes besides autophagy in organisms from yeast to humans, including repression of ribosome biogenesis and protein translation, and transcriptional induction of compensatory metabolic pathways¹³. These probably contribute to the complications seen with long-term rapamycin use, such as immunosuppression, which is not compatible with therapy for infectious diseases. Accordingly, we are aiming to identify safer ways of inducing autophagy, by identifying mTOR substrates regulating autophagy, compounds that enhance the activity of rapamycin, or compounds acting via mTOR-independent pathways.

Here we have identified novel enhancers of mammalian autophagy by starting with a small-molecule screen in yeast¹⁴. We reasoned that a small-molecule screen would uncover enhancers and suppressors of the physiological state induced by rapamycin in yeast, and that the activities of at least some of these modifiers as single agents would be conserved in mammalian systems. From 50,729 compounds screened,

we observed suppressors of the cytostatic effects of rapamycin (small-molecule inhibitors of rapamycin; SMIRs) in yeast in a temporal window that spans 48–72 h; we discerned both fast- and slow-acting SMIRs, but hereafter we do not distinguish between them. Later, at 96 h, we observed enhancers of the cytostatic effects of rapamycin (small-molecule enhancers of rapamycin; SMERs) in wells containing yeast that failed to exit rapamycin-induced growth arrest.

We retested 72 total primary assay positives, from which we identified a structurally nonredundant set of 21 SMIRs (4–24) and 12 SMERs (25–36) (**Supplementary Fig. 1a** online). Further characterization of these SMIRs and SMERs in yeast is described in **Supplementary Methods** and **Supplementary Figure 1b–f** online.

Although these SMIRs and SMERs were discovered as modulators of the effects of rapamycin on yeast growth, we tested whether they were also modulators of mammalian autophagy. We screened all the yeast primary assay positives in mammalian cells (including hits that were excluded from the above analyses in yeast because of their poor potency) in the absence of rapamycin for their potential to induce clearance of the autophagy substrate A53T α -synuclein. We used a stable doxycycline-inducible PC12 cell line expressing A53T mutant α -synuclein, in which the transgene expression is first induced by adding doxycycline and then switched off by removing doxycycline

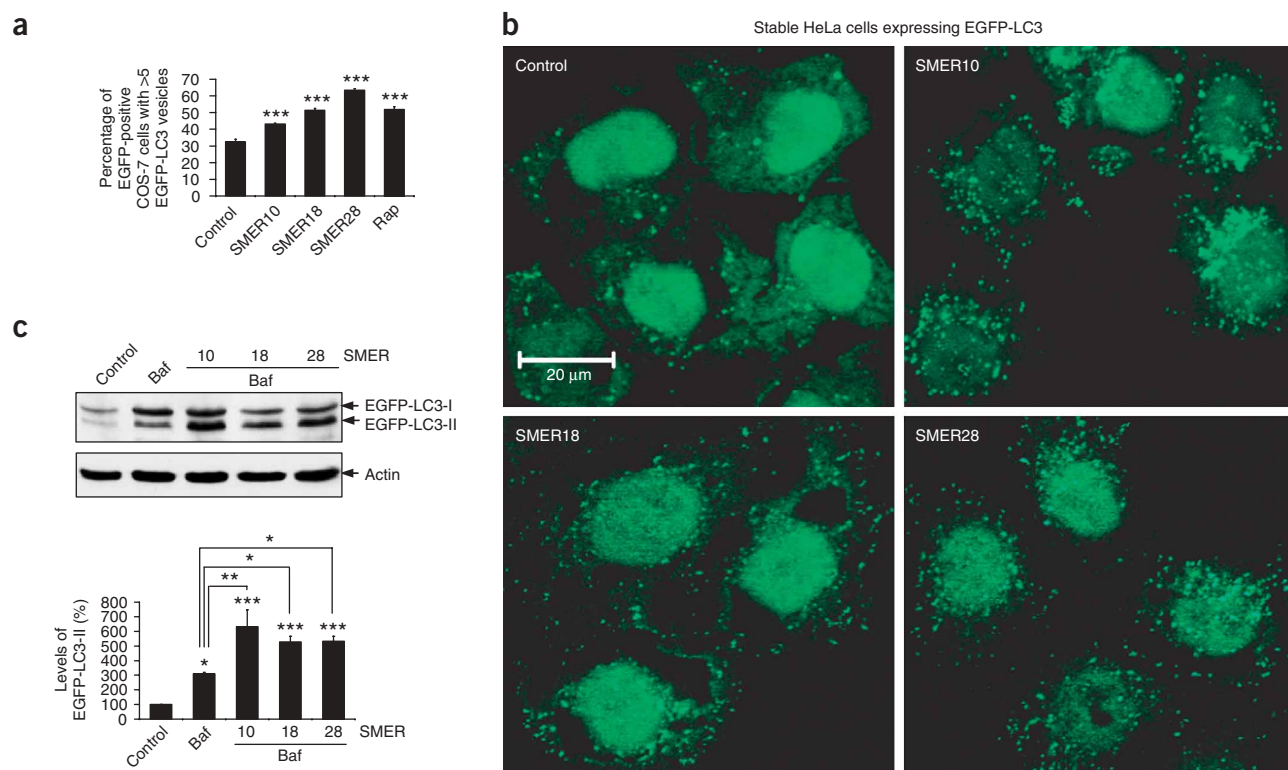


Figure 2 SMERs 10, 18 and 28 induce autophagy in mammalian cells. **(a)** COS-7 cells transfected with EGFP-LC3 construct for 4 h were treated with DMSO (control), 0.2 μ M rapamycin (positive control), 47 μ M SMER10, 43 μ M SMER18 or 47 μ M SMER28 for 16 h, and analyzed by fluorescence microscopy. The effects of treatment on the percentage of EGFP-positive cells with >5 EGFP-LC3 vesicles are shown. Error bars denote s.e.m. $P < 0.0001$ (all SMERs). **(b)** HeLa cells stably expressing EGFP-LC3 were treated with DMSO (control), 47 μ M SMER10, 43 μ M SMER18 or 47 μ M SMER28 for 24 h. Confocal sections show cells containing EGFP-positive autophagic vesicles. Nuclei are stained with DAPI. Bar, 20 μ M. **(c)** HeLa cells stably expressing EGFP-LC3 were treated for 4 h with DMSO (control) or 200 nM bafilomycin A1 (Baf), or with 200 nM bafilomycin A1 and 47 μ M SMER10, 43 μ M SMER18 or 47 μ M SMER28. Cells were left untreated or pretreated with SMERs for 24 h before adding bafilomycin A1. Levels of EGFP-LC3-II were determined by immunoblotting with antibody against EGFP (above) and densitometry analysis relative to actin (below). Error bars denote s.e.m. $P = 0.0259$ (baf), $P < 0.0001$ (SMER10), $P = 0.0003$ (SMER18 and SMER28) versus control; $P = 0.0025$ (SMER10), $P = 0.0218$ (SMER18), $P = 0.0195$ (SMER28) versus bafilomycin A1. *** $P < 0.001$; ** $P < 0.01$; * $P < 0.05$.

from the medium⁵. If the transgene expression level is measured at 24 h after switching off expression after an initial induction period of 48 h, one can assess whether specific agents alter the clearance of the transgene product, as the amount of transgene product decays when synthesis is stopped⁵. Notably, we observed that 13 SMIRs (14–18, 19a, 19b, 22, 23, 29a, 29b, 30 and 31) slowed the clearance of this autophagy substrate, whereas 4 SMERs (10, 16, 18 and 28) enhanced its clearance (Supplementary Fig. 2a–d online; numbering of SMERs and SMIRs here refers to the experimental numbering scheme based on the order in which the compounds were discovered). We categorized SMIRs as possible inhibitors of autophagy if they increased A53T α -synuclein levels by 40–50% or more. Likewise, we categorized SMERs as possible enhancers of autophagy if they reduced A53T α -synuclein levels to 50% or lower than the control (Supplementary Fig. 2a–d).

We then concentrated on the autophagy-inducing SMERs, which may have the greatest immediate utility as drug leads for neurodegenerative diseases (Fig. 1a). We confirmed that SMERs 10 (27), 18 (30) and 28 (36) substantially enhance A53T α -synuclein clearance in PC12 cells; this effect was independent of rapamycin treatment, and efficacy was observed with the doses used in the yeast screen and also at lower concentrations (Fig. 1b). In all subsequent experiments with these compounds alone, we used the concentrations used in the yeast screen.

We next studied the effect of these SMERs on another autophagy substrate: mutant huntingtin^{3,4}. SMERs 10, 18 and 28 reduced aggregation and cell death caused by enhanced green fluorescent protein (EGFP)-tagged huntingtin exon 1 with 74 polyQ repeats (EGFP-HDQ74) in COS-7 cells (Fig. 1c). We excluded SMER 16 (subsequently redesignated SMIR 33 because additional retesting revealed it to be a suppressor of the cytostatic effects of rapamycin) from our subsequent experiments as it was toxic in COS-7 and other cell lines at the concentration that enhanced the clearance of A53T α -synuclein in PC12 cells (data not shown). No overt toxicity was observed with SMERs 10, 18 and 28 (see Supplementary Methods).

We confirmed that this reduction of EGFP-HDQ74 aggregation occurs via autophagy using autophagy-competent mouse embryonic fibroblasts (MEFs) (*Atg5*^{+/+}) or matched MEFs lacking the essential autophagy gene *Atg5* (*Atg5*^{-/-})¹⁵. EGFP-HDQ74 aggregation was significantly ($P < 0.0001$) increased in untreated *Atg5*^{-/-} (autophagy-deficient) cells compared with untreated *Atg5*^{+/+} cells, as mutant huntingtin is an autophagy substrate (Supplementary Fig. 3a online). SMERs 10, 18 and 28 significantly reduced EGFP-HDQ74 aggregation in *Atg5*^{+/+} cells, but not in *Atg5*^{-/-} cells (Fig. 1d). Thus, these SMERs can only reduce mutant huntingtin aggregation in autophagy-competent cells. Indeed, these SMERs decreased EGFP-HDQ74 aggregation in cells constitutively treated with the proteasome inhibitor

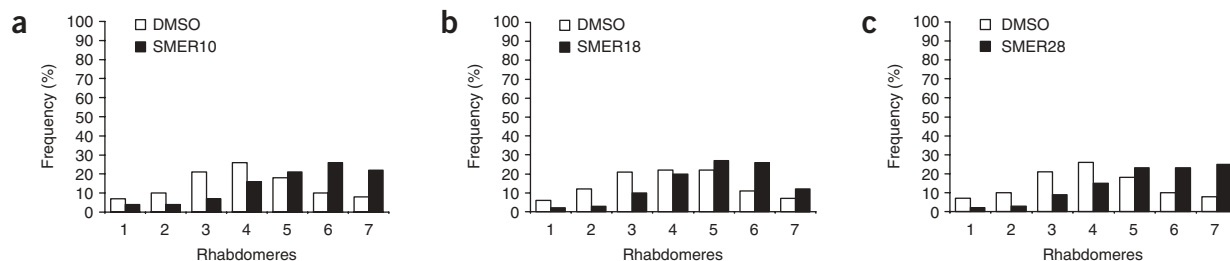


Figure 3 SMERs 10, 18 and 28 protect against neurodegeneration in *D. melanogaster* model of Huntington's disease. (**a–c**) Flies treated with 100 μ M SMER10 (**a**), 200 μ M SMER18 (**b**) or 100 μ M SMER28 (**c**) show a shift in the distribution of the number of rhabdomeres compared with flies treated with DMSO (control) alone (2 d after eclosion). Rhabdomere counts from all three independent experiments are included. $n = 600$ ommatidia (SMER10), $n = 1,500$ ommatidia (SMER18) and $n = 600$ ommatidia (SMER28). Mann-Whitney test values $P < 0.0001$ (all SMERs). Student's t -test (1-tailed) $P = 0.005$ (SMER10), $P = 0.004$ (SMER18), $P = 0.03$ (SMER28) comparing means of distributions from independent experiments. These SMER concentrations cause no overt toxicity to flies (see **Supplementary Methods**). Distributions of DMSO-treated flies may vary when SMERs are treated in different experiments at different times. For instance, an individual experiment may have lasted slightly longer or shorter and photoreceptor degeneration is progressive and time-dependent.

lactacystin¹⁶ (37) (which targets the main alternate route for mutant huntingtin clearance) (Fig. 1e).

We next assessed the effect of these SMERs on autophagy by transfecting COS-7 cells with the microtubule-associated protein 1 light chain 3 (LC3) fused to EGFP (EGFP-LC3). LC3 (and EGFP-LC3) localizes only to autophagic membranes, not to other membrane structures, and serves as a specific marker for autophagosomes¹⁷. As EGFP-LC3 overexpression does not affect autophagic activity, the number of EGFP-LC3 vesicles has frequently been used to assess autophagosome number, and therefore to make inferences about autophagic activity¹⁸. SMERs 10, 18 and 28 significantly ($P < 0.0001$) increased the proportion of cells with EGFP-LC3 vesicles compared with control (DMSO-treated) cells (Fig. 2a).

We then tested for autophagy induction by the SMERs in an EGFP-LC3-expressing stable HeLa cell line¹⁹. Treatment of these cells with SMERs 10, 18 and 28 led to overt EGFP-LC3 vesicle formation compared with the control cells (Fig. 2b); note that some cell types, for example, HeLa cells, have more autophagosomes per cell than other cell types, for example, COS-7 cells.

Endogenous LC3 is processed post-translationally into LC3-I, which is cytosolic. LC3-I is in turn converted to LC3-II, which associates with autophagosome membranes¹⁷. LC3-II can accumulate as a result of increased upstream autophagosome formation, and also if there is impaired downstream autophagosome-lysosome fusion. To distinguish between these two possibilities, we assayed LC3-II in the presence of bafilomycin A1 (38), which blocks downstream autophagosome-lysosome fusion²⁰. Bafilomycin A1 increased EGFP-LC3-II levels in stable HeLa cells, as expected (Fig. 2c). The dose of bafilomycin A1 used is saturating for LC3-II levels in this assay, and no further increases in LC3-II were observed when we treated cells with bafilomycin A1 and agents that block autophagosome-lysosome fusion via independent mechanisms (such as the dynein inhibitor erythro-9-[3-(2-hydroxy-nonyl)] adenine (EHNA)²¹) (39) (data not shown). However, autophagy inducers increase LC3-II levels even when cells are constitutively treated with this dose of bafilomycin A1⁸. SMERs 10, 18 and 28 substantially increased EGFP-LC3-II levels in the presence of bafilomycin A1, compared with bafilomycin A1 alone, which strongly argues that the increased numbers of autophagosomes induced by these SMERs are a result of enhanced autophagosome formation (Fig. 2c).

We tested the potential of the three autophagy-enhancing SMERs to function *in vivo* using a *D. melanogaster* model of HD expressing the

first 171 residues of mutant huntingtin with 120 polyQ repeats in photoreceptors, using the pseudopupil technique (see Methods). The compound eyes in flies consist of several hundred ommatidia, each containing eight photoreceptor neurons with light-gathering parts called rhabdomeres, seven of which can be visualized using the pseudopupil technique. This method assesses the number of visible rhabdomeres by light microscopy and has been widely used to quantify the toxicity of proteins with long polyQs in the fly eye^{4,22,23}. The number of visible rhabdomeres in each ommatidium decreases over time in the mutant *D. melanogaster* expressing mutant huntingtin with 120 polyQ repeats in photoreceptors, compared with the wild-type flies or transgenic flies expressing otherwise identical huntingtin with 23 polyQ (wild-type) repeats (where there is no degeneration). SMERs 10, 18 and 28 protected against neurodegeneration in *D. melanogaster* expressing mutant huntingtin, compared with flies treated with the vehicle (DMSO) (Fig. 3). Thus, these SMERs protect against polyglutamine toxicity *in vivo* in neurons. These SMERs are not toxic for *D. melanogaster* development or for *D. melanogaster* photoreceptors at the relevant concentrations we have used to protect against polyQ toxicity (see **Supplementary Methods**).

We next tested whether these autophagy-inducing SMERs act primarily via the pathway that is negatively regulated by mTOR. mTOR kinase activity can be inferred by the levels of phosphorylation of its substrates, ribosomal S6 protein kinase (S6K1, also known as p70S6K) and eukaryotic initiation factor 4E-binding protein 1 (4E-BP1), at Thr389 and Thr37/46, respectively²⁴. Though rapamycin substantially reduced the amounts of total p70S6K and 4E-BP1 that were phosphorylated, SMERs 10, 18 and 28 had no such effects (Supplementary Fig. 3b,c). However, the proportion of total S6K1 that is phosphorylated in the presence of SMER 28 may be slightly less than in the control-treated cells (although the effect is diminished relative to that seen with rapamycin).

The SMERs did not affect the levels of various autophagy regulators, such as Beclin-1 (Atg6), Atg5, Atg7 and Atg12, and they did not enhance conjugation of Atg12 to Atg5, which is a critical step in autophagosome assembly preceding LC3 conjugation (Supplementary Fig. 3d–h). Our data suggest that these SMERs induce mammalian autophagy in an mTOR-independent fashion. However, it is also conceivable that the SMERs impinge upon an unknown component of the mTOR autophagy pathway downstream of mTOR. Whatever the case may be, the increased sensitivity afforded by using

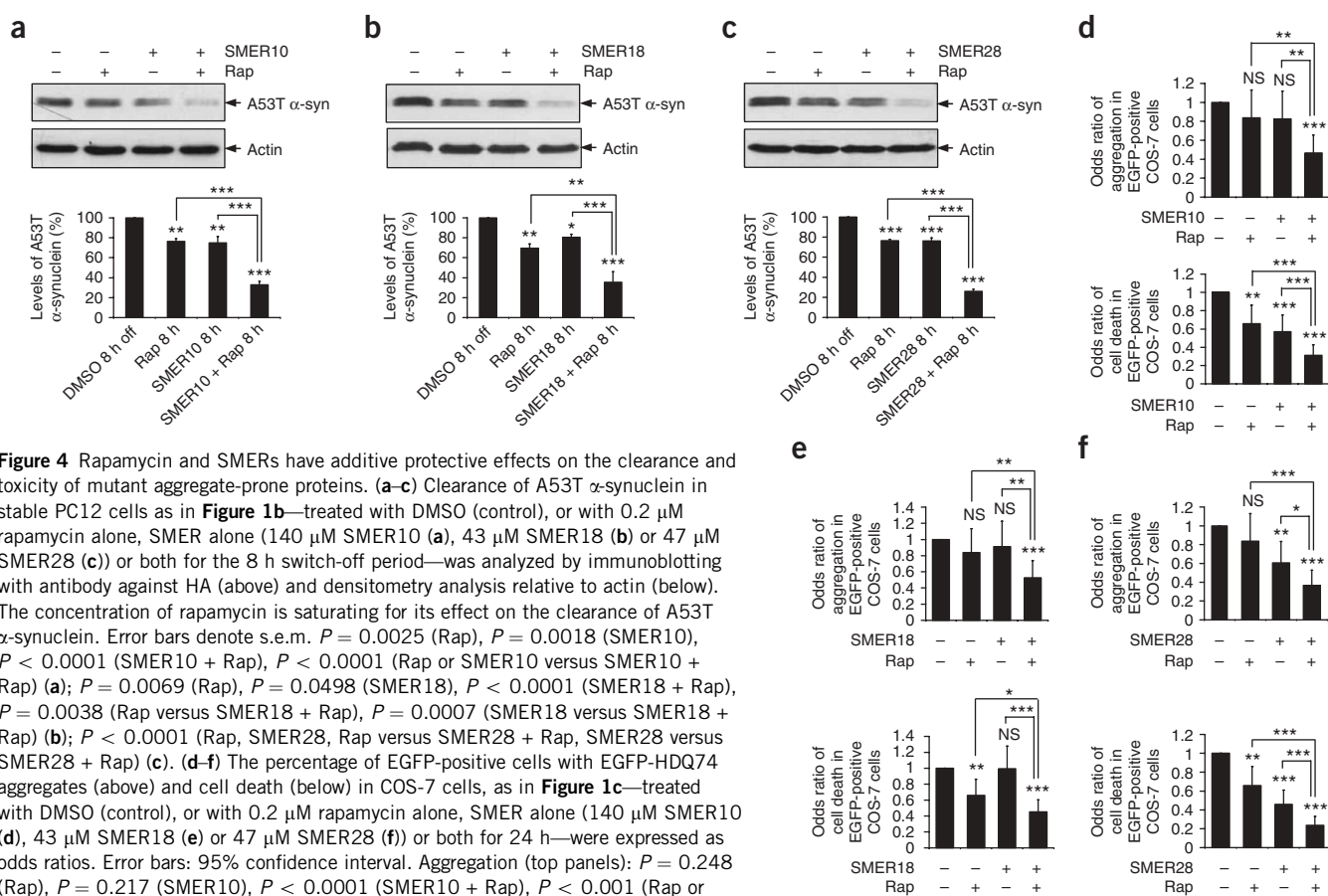


Figure 4 Rapamycin and SMERs have additive protective effects on the clearance and toxicity of mutant aggregate-prone proteins. (**a–c**) Clearance of A53T α -synuclein in stable PC12 cells as in **Figure 1b**—treated with DMSO (control), or with 0.2 μ M rapamycin alone, SMER alone (140 μ M SMER10 (**a**), 43 μ M SMER18 (**b**) or 47 μ M SMER28 (**c**) or both for the 8 h switch-off period—was analyzed by immunoblotting with antibody against HA (above) and densitometry analysis relative to actin (below). The concentration of rapamycin is saturating for its effect on the clearance of A53T α -synuclein. Error bars denote s.e.m. $P = 0.0025$ (Rap), $P = 0.0018$ (SMER10), $P < 0.0001$ (SMER10 + Rap), $P < 0.0001$ (Rap or SMER10 versus SMER10 + Rap) (**a**); $P = 0.0069$ (Rap), $P = 0.0498$ (SMER18), $P < 0.0001$ (SMER18 + Rap), $P = 0.0038$ (Rap versus SMER18 + Rap), $P = 0.0007$ (SMER18 versus SMER18 + Rap) (**b**); $P < 0.0001$ (Rap, SMER28, Rap versus SMER28 + Rap, SMER28 versus SMER28 + Rap) (**c**). (**d–f**) The percentage of EGFP-positive cells with EGFP-HDQ74 aggregates (above) and cell death (below) in COS-7 cells, as in **Figure 1c**—treated with DMSO (control), or with 0.2 μ M rapamycin alone, SMER alone (140 μ M SMER10 (**d**), 43 μ M SMER18 (**e**) or 47 μ M SMER28 (**f**) or both for 24 h—were expressed as odds ratios. Error bars: 95% confidence interval. Aggregation (top panels): $P = 0.248$ (Rap), $P = 0.217$ (SMER10), $P < 0.0001$ (SMER10 + Rap), $P < 0.001$ (Rap or SMER10 versus SMER10 + Rap) (**d**); $P = 0.248$ (Rap), $P = 0.543$ (SMER18), $P < 0.0001$ (SMER18 + Rap), $P = 0.008$ (Rap versus SMER18 + Rap), $P = 0.002$ (SMER18 versus SMER18 + Rap) (**e**); $P = 0.248$ (Rap), $P = 0.002$ (SMER28 versus SMER28 + Rap) (**f**). Cell death (bottom panels): $P = 0.002$ (Rap), $P < 0.0001$ (SMER10, SMER10 + Rap, Rap or SMER10 versus SMER10 + Rap) (**d**); $P = 0.002$ (Rap), $P = 0.948$ (SMER18), $P < 0.0001$ (SMER18 + Rap), $P = 0.015$ (Rap versus SMER18 + Rap), $P < 0.0001$ (SMER18 versus SMER18 + Rap) (**e**); $P = 0.002$ (Rap), $P < 0.0001$ (SMER28, SMER28 + Rap, Rap or SMER28 versus SMER28 + Rap) (**f**). Note that we have treated cells for a shorter time in this experiment (24 h), compared with **Figure 1c** (48 h). This probably accounts for the failure of the protective trends of rapamycin and some of the SMERs to reach significance for aggregation on their own in some of the experiments. *** $P < 0.001$; ** $P < 0.01$; * $P < 0.05$; NS, nonsignificant.

cellular growth as a screening readout may be one reason why not all SMERs or SMIRs that emerged from the primary screen modulate autophagy, which is but one of many cellular pathways downstream of TOR. Unfortunately, it is difficult to test these hypotheses directly, as the mTOR substrates and the relevant downstream effectors that mediate mammalian autophagy have not been identified.

These SMERs did not cause accumulation of the Ub^{G76V}-EGFP degon, a specific proteasome substrate²⁵, in contrast to the proteasome inhibitor lactacystin (**Supplementary Fig. 3i**). Thus, these SMERs do not induce autophagy by causing major impairments in the ubiquitin/proteasome pathway²⁶.

We next investigated whether these SMERs, which enhance rapamycin's cytostatic effects in yeast, could also enhance the clearance of mutant proteins by rapamycin in mammalian cells. We assessed the clearance of A53T α -synuclein in stable PC12 cells at an early time point of 8 h (instead of 24 h as shown earlier), at which we do not see substantial reductions of the levels of this autophagy substrate when the cells are treated with either of the compounds alone. SMERs 10, 18 and 28 and rapamycin all had small but significant effects even at this early time point (**Fig. 4a–c**). Combined treatment of SMERs 10, 18 or 28 with rapamycin substantially enhanced the effects of rapamycin

(or the SMER) alone on A53T α -synuclein clearance (**Fig. 4a–c**). Here, we have used saturating doses of rapamycin⁶ to demonstrate the combined effects.

We further confirmed the enhanced protective effect that results from dual treatment in mutant huntingtin-expressing COS-7 cells. Treatment with SMERs 10, 18 or 28 and rapamycin had an additive effect in reducing EGFP-HDQ74 aggregates and toxicity, compared with the single treatments of rapamycin or the SMERs (**Fig. 4d–f**).

We next performed limited structure-activity relationship (SAR) analyses on SMERs 10, 18 and 28. We tested three commercially available structural analogs of SMER10 (**40–42**) and 12 commercially available structural analogs of SMER18 (**43–54**), and we synthesized 11 structural analogs of SMER28 (**55–64**). Note that SMER28e is the same as the parent compound. We first screened for clearance of A53T α -synuclein in stable PC12 cells treated with these structural analogs alone. Structural analogs that retained the ability to induce clearance of A53T α -synuclein were then further tested for their ability to reduce mutant huntingtin aggregation in COS-7 cells. We found that one SMER10 analog (SMER10a), seven SMER18 analogs (SMER18a and SMER18c–SMER18h) and ten SMER28 analogs (SMER28a and SMER28c–SMER28k) all substantially enhanced the clearance of the

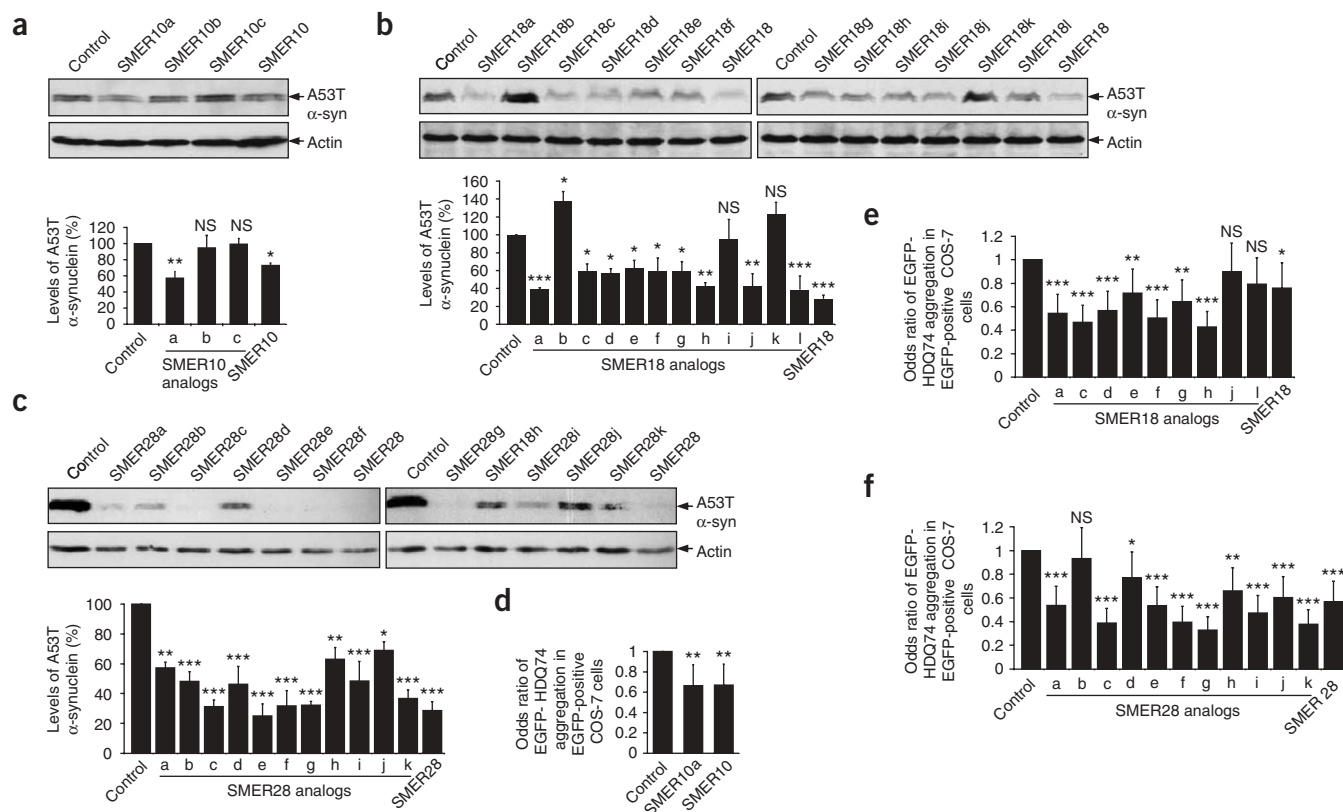


Figure 5 Screen of chemical analogs of autophagy-inducing SMERs for their protective effects on the clearance and aggregation of mutant proteins. (a–c) Clearance of A53T α-synuclein in stable PC12 cells as in **Figure 1b**—treated for 24 h with either DMSO (control), or with 47 μM SMER10 and its analogs (SMER10a–c) (a), 43 μM SMER18 and its analogs (SMER18a–l) (b), or 47 μM SMER28 and its analogs (SMER28a–k) (c)—was analyzed by immunoblotting with anti-HA antibody (above) and densitometry analysis relative to actin (below). All the analogs were used in the cell culture medium at 1:400 dilution of 5 mg ml^{−1} stock solution (in DMSO). Error bars denote s.e.m. $P = 0.0058$ (SMER10a), $P = 0.6736$ (SMER10b), $P = 0.9507$ (SMER10c), $P = 0.0481$ (SMER10) (a); $P = 0.0006$ (SMER18a), $P = 0.0249$ (SMER18b), $P = 0.0167$ (SMER18c), $P = 0.0117$ (SMER18d), $P = 0.0269$ (SMER18e), $P = 0.0165$ (SMER18f), $P = 0.0148$ (SMER18g), $P = 0.0011$ (SMER18h), $P = 0.7369$ (SMER18i), $P = 0.0012$ (SMER18j), $P = 0.1531$ (SMER18k), $P = 0.0006$ (SMER18l), $P = 0.0001$ (SMER18) (b); $P = 0.0014$ (SMER28a), $P = 0.0002$ (SMER28b), $P = 0.0001$ (SMER28c), $P = 0.0048$ (SMER28d), $P = 0.0002$ (SMER28e), $P = 0.0002$ (SMER28f), $P = 0.0162$ (SMER28g), $P < 0.0001$ (SMER28h), $P = 0.0001$ (SMER28i), $P = 0.0001$ (SMER28j), $P = 0.0001$ (SMER28k), $P = 0.0001$ (SMER28l), $P = 0.0001$ (SMER28) (c). (d–f) The percentage of EGFP-positive cells with EGFP-HDQ74 aggregates in COS-7 cells as in **Figure 1c**—treated for 48 h with either DMSO (control), or with 47 μM SMER10 and its analog (SMER10a) (d), 43 μM SMER18 and its analogs (SMER18a, SMER18c–h, SMER18j, SMER18l) (e), or 47 μM SMER28 and its analogs (SMER28a–k) (f)—were expressed as odds ratios. All the analogs were used in the cell culture medium at 1:400 dilution of 5 mg ml^{−1} stock solution (in DMSO). Error bars: 95% confidence interval. $P = 0.003$ (SMER10a), $P = 0.004$ (SMER10) (d); $P < 0.0001$ (SMER18a, SMER18c, SMER18d, SMER18f, SMER18h), $P = 0.009$ (SMER18e), $P = 0.001$ (SMER18g), $P = 0.382$ (SMER18i), $P = 0.067$ (SMER18j), $P = 0.031$ (SMER18l) (e); $P < 0.0001$ (SMER28a, SMER28c, SMER28e–g, SMER28i–k, SMER28l), $P = 0.574$ (SMER28b), $P = 0.041$ (SMER28d), $P = 0.002$ (SMER28h) (f). *** $P < 0.001$; ** $P < 0.01$; * $P < 0.05$; NS, nonsignificant.

A53T α-synuclein and reduced huntingtin aggregation, though in most cases not significantly better than the parent compounds (**Fig. 5**). Thus, we have identified further candidates having potential for therapeutic development.

SMER10 is an aminopyrimidone. The pyrimidone functionality of SMER10 is important for its autophagy-inducing activity, because substitution of a bulky phenyl group at the 2 position (SMER10b (41)), or creating a fused tetrazole (SMER10c (42)), nearly abolishes activity (**Fig. 5a**). However, removal of the amino group at the 3 position, thereby yielding hypoxanthine (SMER10a (40)), may slightly increase activity compared with the parent compound (**Fig. 5a**).

SMER18 is a vinylogous amide. The SMER18 analogs assess the tolerance of the two terminal aromatic rings to substitutions (**Fig. 5b**). For example, changing the hydroxyl group from the *meta* position to either the *para* (SMER18g (49)) or the *ortho* (SMER18f (48)) positions reduces but does not abolish activity; yet removing the hydroxyl

group (SMER18i (51)) does abolish activity, which indicates its importance for activity (**Fig. 5b**).

SMER28 is a bromo-substituted quinazoline. A similar SAR pattern emerges here: most substitutions are well tolerated individually, multiple concurrent substitutions fare worse and none of the analogs are significantly more potent than the parent compound (**Fig. 5c**). Notably, two analogs of SMER28 (SMER28h (63) and SMER28i (64)) that have been functionalized in a way suitable for affinity chromatography are also active.

In conclusion, we have developed a high-throughput screening strategy for identifying small-molecule modulators of mammalian autophagy, as SMERs in yeast seem to act as autophagy inducers on their own in mammalian cells. Autophagy inducers may have value for a range of both neurodegenerative and infectious diseases. Autophagy inhibitors may also have use in the treatment of certain cancers.

METHODS

Mammalian cell lines. Cell lines used were COS-7; HeLa; stable HeLa cells expressing EGFP-LC3¹⁹ or Ub^{G76V}-EGFP degran²⁵; wild-type Atg5^{+/+} and Atg5^{-/-} MEFs¹⁵; and inducible PC12 stable cell line expressing HA-tagged A53T α -synuclein mutant⁵. For details of cell culture and transfection, see **Supplementary Methods**.

Quantification of aggregate formation and cell death. Approximately 200 EGFP-positive cells per coverslip were counted by fluorescence microscopy for the proportion of cells with EGFP-HDQ74 aggregates, as described previously^{3,6,8,27}. Nuclei were stained with 4',6-diamidino-2-phenylindole (DAPI) and those showing apoptotic morphology were considered abnormal. Experiments were done in triplicate and with the scorer blinded to treatment.

Western blot analysis. Cell pellets were lysed on ice in Laemmli buffer (62.5 mM Tris-HCl pH 6.8, 5% β -mercaptoethanol, 10% glycerol and 0.01% bromophenol blue) for 30 min in presence of protease inhibitors (Roche Diagnostics). Primary antibodies include anti-EGFP (8362-1, Clontech), anti-HA (12CA5, Covance), anti-mTOR (2972), anti-phospho-mTOR (Ser2448) (2971), anti-p70 S6 kinase (9202), anti-phospho-p70 S6 kinase (Thr389) (9206), anti-4E-BP1 (9452), anti-phospho-4E-BP1 (Thr37/46) (9459) (all from Cell Signaling Technology), anti-beclin-1 (3738, Cell Signaling), anti-Atg5 (ab19130, Abcam), anti-Atg7 (600-401-487, Rockland), anti-Atg12 (36-6400, Zymed Laboratories), anti-actin (A2066, Sigma). Blots were probed with anti-mouse or anti-rabbit IgG-HRP and visualized using an ECL detection kit (Amersham).

Clearance of A53T α -synuclein. Stable inducible PC12 cell line expressing A53T α -synuclein mutant was induced with 1 μ g ml⁻¹ doxycycline (Sigma) for 48 h and the transgene expression was switched off by removing doxycycline from the medium⁵. Cells were treated with or without compounds for time points as indicated in experiments. Clearance of A53T α -synuclein was measured by immunoblotting with antibody against HA, and densitometry analysis measurements were made relative to actin.

D. melanogaster methods. Fly culture and crosses were carried out at 25 °C and at 70% humidity, using Instant Fly Food (Philip Harris) unless otherwise stated. Flies were raised with a 12-h light:12-h dark cycle. Aliquots of SMERs in DMSO, or DMSO alone, were added to the water that was used to prepare the instant fly food.

Virgin female flies of genotype *y w; gmr-httNterm(1-171)Q120 (gmrQ120)*²² were mated with isogenized *w¹¹¹⁸* males²⁸ in food vials for 48 h. Flies were then transferred to vials containing instant fly food with either SMERs in DMSO or DMSO alone. Progeny were collected 0–4 h after eclosion, kept on food of the same composition as they had been reared on, and scored for photoreceptor degeneration using the pseudopupil technique²⁹ 2 d after eclosion.

Statistical analysis. Pooled estimates for the changes in aggregate formation or cell death, resulting from perturbations assessed in multiple experiments, were calculated as odds ratios with 95% confidence intervals. Odds ratios and *P* values were determined by unconditional logistical regression analysis, using the general log-linear analysis option of SPSS 9 software (SPSS). Densitometry analysis on the immunoblots was done by Scion Image Beta 4.02 software (Scion Corporation) from three independent experiments (*n* = 3). Significance for the clearance of mutant proteins was determined by factorial ANOVA test using Statview software, version 4.53 (Abacus Concepts), in which the control condition was set to 100%. The *y*-axis values are shown in percentage (%) and the error bars denote s.e.m. ****P* < 0.001; ***P* < 0.01; **P* < 0.05; NS, nonsignificant. For further details, see **Supplementary Methods**.

SMER28 structural analog synthesis. See **Supplementary Methods** for details.

Other methods. See **Supplementary Methods** for details of yeast strains and media, primary screen, dose responses and selectivity profiling, characterizations of SMERs and SMIRs in yeast, plasmid constructs, mammalian cell culture and transfection, microscopy, detailed statistical analysis (for counting

aggregation, cell death, EGFP-LC3 vesicles and densitometry on immunoblots), toxicity analyses and synthesis of SMER28 analogs.

Note: Supplementary information and chemical compound information is available on the Nature Chemical Biology website.

ACKNOWLEDGMENTS

We thank T. Yoshimori (Japanese National Institute of Genetics) for the EGFP-LC3 construct, N. Mizushima (Tokyo Metropolitan Institute of Medical Science) for Atg5 and HA-Atg12 constructs, and wild-type and Atg5-deficient MEFs, A.M. Tolkskovy (University of Cambridge) for EGFP-LC3 HeLa stable cell line and N.P. Dantuma (Karolinska Institutet) for Ub^{G76V}-EGFP degran HeLa stable cell line. We thank the staff of the Broad Institute Chemical Biology Program (formerly the Institute for Chemistry and Chemical Biology), B. Ravikumar, A. Williams, L. Jahreis and R. Walker (University of Cambridge) for technical assistance; and S. Haggarty for comments and discussion. This work was supported in part with federal funds from the US National Cancer Institute's Initiative for Chemical Genetics, National Institutes of Health, under Contract No. N01-CO-12400. We are grateful for a Wellcome Trust Senior Fellowship in Clinical Science (D.C.R.), an MRC programme grant, an EU Framework VI (EUROSCA) grant (D.C.R.) and the US National Institute of General Medicine Sciences GM38627 (S.L.S.) for additional funding. S.L.S. is an investigator at the Howard Hughes Medical Institute.

AUTHOR CONTRIBUTIONS

S.S. and E.O.P. designed, performed and analyzed experiments and helped write the paper; S.I., S.P., A.C., R.L.M., J.A.W. and T.A.L. performed and analyzed experiments; C.J.O. designed and analyzed experiments; S.L.S. and D.C.R. designed and analyzed experiments and helped write the paper.

COMPETING INTERESTS STATEMENT

The authors declare no competing financial interests.

Published online at <http://www.nature.com/naturechemicalbiology>

Reprints and permissions information is available online at <http://npg.nature.com/reprintsandpermissions>

- Klionsky, D.J. & Emr, S.D. Autophagy as a regulated pathway of cellular degradation. *Science* **290**, 1717–1721 (2000).
- Rubinsztein, D.C., Gestwicki, J.E., Murphy, L.O. & Klionsky, D.J. Potential therapeutic applications of autophagy. *Nat. Rev. Drug Discov.* **6**, 304–312 (2007).
- Ravikumar, B., Duden, R. & Rubinsztein, D.C. Aggregate-prone proteins with polyglutamine and polyalanine expansions are degraded by autophagy. *Hum. Mol. Genet.* **11**, 1107–1117 (2002).
- Ravikumar, B. *et al.* Inhibition of mTOR induces autophagy and reduces toxicity of polyglutamine expansions in fly and mouse models of Huntington disease. *Nat. Genet.* **36**, 585–595 (2004).
- Webb, J.L., Ravikumar, B., Atkins, J., Skepper, J.N. & Rubinsztein, D.C. α -synuclein is degraded by both autophagy and the proteasome. *J. Biol. Chem.* **278**, 25009–25013 (2003).
- Sarkar, S. *et al.* Lithium induces autophagy by inhibiting inositol monophosphatase. *J. Cell Biol.* **170**, 1101–1111 (2005).
- Rubinsztein, D.C. Lessons from animal models of Huntington's disease. *Trends Genet.* **18**, 202–209 (2002).
- Sarkar, S., Davies, J.E., Huang, Z., Tunnacliffe, A. & Rubinsztein, D.C. Trehalose, a novel mTOR-independent autophagy enhancer, accelerates the clearance of mutant huntingtin and α -synuclein. *J. Biol. Chem.* **282**, 5641–5652 (2007).
- Berger, Z. *et al.* Rapamycin alleviates toxicity of different aggregate-prone proteins. *Hum. Mol. Genet.* **15**, 433–442 (2006).
- Gutierrez, M.G. *et al.* Autophagy is a defense mechanism inhibiting BCG and *Mycobacterium tuberculosis* survival in infected macrophages. *Cell* **119**, 753–766 (2004).
- Nakagawa, I. *et al.* Autophagy defends cells against invading group A *Streptococcus*. *Science* **306**, 1037–1040 (2004).
- Talloczy, Z., Virgin, H.W.T. & Levine, B. PKR-dependent autophagic degradation of herpes simplex virus type 1. *Autophagy* **2**, 24–29 (2006).
- Sarbasov, D.D., Ali, S.M. & Sabatini, D.M. Growing roles for the mTOR pathway. *Curr. Opin. Cell Biol.* **17**, 596–603 (2005).
- Huang, J. *et al.* Finding new components of the target of rapamycin (TOR) signaling network through chemical genetics and proteome chips. *Proc. Natl. Acad. Sci. USA* **101**, 16594–16599 (2004).
- Mizushima, N. *et al.* Dissection of autophagosome formation using Apg5-deficient mouse embryonic stem cells. *J. Cell Biol.* **152**, 657–668 (2001).
- Fenteany, G. *et al.* Inhibition of proteasome activities and subunit-specific amino-terminal threonine modification by lactacystin. *Science* **268**, 726–731 (1995).
- Kabeya, Y. *et al.* LC3, a mammalian homologue of yeast Apg8p, is localized in autophagosome membranes after processing. *EMBO J.* **19**, 5720–5728 (2000).
- Mizushima, N. Methods for monitoring autophagy. *Int. J. Biochem. Cell Biol.* **36**, 2491–2502 (2004).

19. Bampton, E.T.W., Goemans, C.G., Niranjana, D., Mizushima, N. & Tolkovsky, A.M. The dynamics of autophagy visualised in live cells: from autophagosome formation to fusion with endo/lysosomes. *Autophagy* **1**, 23–36 (2005).
20. Yamamoto, A. *et al.* Bafilomycin A1 prevents maturation of autophagic vacuoles by inhibiting fusion between autophagosomes and lysosomes in rat hepatoma cell line, H-4-II-E cells. *Cell Struct. Funct.* **23**, 33–42 (1998).
21. Ekstrom, P. & Kanje, M. Inhibition of fast axonal transport by erythro-9-[3-(2-hydroxy-nonyl)]adenine. *J. Neurochem.* **43**, 1342–1345 (1984).
22. Jackson, G.R. *et al.* Polyglutamine-expanded human huntingtin transgenes induce degeneration of *Drosophila* photoreceptor neurons. *Neuron* **21**, 633–642 (1998).
23. Marsh, J.L. & Thompson, L.M. *Drosophila* in the study of neurodegenerative disease. *Neuron* **52**, 169–178 (2006).
24. Schmelzle, T. & Hall, M.N. TOR, a central controller of cell growth. *Cell* **103**, 253–262 (2000).
25. Dantuma, N.P., Lindsten, K., Glas, R., Jellne, M. & Masucci, M.G. Short-lived green fluorescent proteins for quantifying ubiquitin/proteasome-dependent proteolysis in living cells. *Nat. Biotechnol.* **18**, 538–543 (2000).
26. Iwata, A., Riley, B.E., Johnston, J.A. & Kopito, R.R. HDAC6 and microtubules are required for autophagic degradation of aggregated huntingtin. *J. Biol. Chem.* **280**, 40282–40292 (2005).
27. Narain, Y., Wyttenbach, A., Rankin, J., Furlong, R.A. & Rubinsztein, D.C. A molecular investigation of true dominance in Huntington's disease. *J. Med. Genet.* **36**, 739–746 (1999).
28. Ryder, E. *et al.* The DrosDel collection: a set of P-element insertions for generating custom chromosomal aberrations in *Drosophila melanogaster*. *Genetics* **167**, 797–813 (2004).
29. Franceschini, N. in *Information Processing in the Visual System of Drosophila* (ed. Wehner, R.) 75–82 (Springer, Berlin, 1972).